Role of external and internal perturbations on the ferromagnetic phase transition in $Sm_{0.52}Sr_{0.48}MnO_3$

P. Sarkar,[1,2,*] P. Mandal,[2] K. Mydeen,[3] A. K. Bera,[4] S. M. Yusuf,[4] S. Arumugam,[3] C. Q. Jin,[5] T. Ishida,[6] and S. Noguchi[6]

[1]*Department of Physics, Serampore College, Serampore 712 201, India*

[2]*Saha Institute of Nuclear Physics, 1/AF Bidhannagar, Calcutta 700 064, India*

[3]*Centre for High Pressure Research, School of Physics, Bharathidasan University, Tiruchirappalli 620 024, India*

[4]*Solid State Physics Division, Bhabha Atomic Research Centre, Mumbai 400 085, India*

[5]*Beijing National Laboratory for Condensed Matter Physics, Institute of Physics, Chinese Academy of Sciences, Beijing 100 080, China*

[6]*Department of Physics and Electronics, Osaka Prefecture University, 1-1, Gakuen-cho, Naka-ku, Sakai, Osaka 599 8531, Japan*

(Received 10 December 2008; revised manuscript received 6 February 2009; published 28 April 2009)

We report on the magnetic field (H), hydrostatic pressure (P), and doping dependence of the order of the ferromagnetic (FM) to paramagnetic (PM) phase transition in $Sm_{0.52}Sr_{0.48}MnO_3$ single crystal. It has been shown that ($H_{cr} \approx 4$ T, $T_{cr} \approx 160$ K) is a critical point below which FM to PM phase transition is first order in nature accompanied by a sharp drop in resistivity and magnetization with thermal hysteresis. Below the critical point, these parameters also show field-induced metamagnetic transition along with hysteresis between the increasing and decreasing fields. All these signatures of first-order FM transition disappear above the critical point and the transition becomes a crossover. The effect of P on the nature of FM-PM transition is quite similar to that of H and the corresponding critical point, where the character of FM transition that changes from first to second order is ($P_{cr} \approx 2.5$ GPa, $T_{cr} \approx 160$ K). We have also determined the location of critical point expressed in terms of Nd concentration (y) of $(Sm_{1-y}Nd_y)_{0.52}Sr_{0.48}MnO_3$ and found that the transition changes to second order at ($y_{cr} \approx 0.4$, $T_{cr} \approx 175$ K). The change in the character of FM transition with the application of external (H and P) and internal (Nd concentration) perturbations has been explained within the framework of the formation of polarons.

DOI: 10.1103/PhysRevB.79.144431 PACS number(s): 75.30.Kz

I. INTRODUCTION

Perovskite-type manganites $R_{1-x}A_xMnO_3$ (R: rare-earth ions; A: alkaline earth ions) exhibit various fundamental phenomena of current interest including colossal magnetoresistance, charge and orbital ordering, phase separation, metal-insulator transition (MIT), and first-order ferromagnetic (FM) to paramagnetic (PM) phase transition in particular.[1–4] Most of them are collective phenomena arising from the strong interplay among spin, charge, orbital, and lattice degrees of freedom. The effect of these competitive interactions becomes much stronger when the bandwidth of the system is small. Several studies on narrowband manganites have revealed that the first-order nature of phase transition can be preserved in presence of quenched disorder that arises mainly due to the size mismatch between R and A ions.[1–7] Thus, one can introduce a large local disorder in the system by selecting the rare-earth element of smaller ionic radius and the alkaline earth element of larger ionic radius. As the ionic radius of Sm and Sr differs significantly, the value of quenched disorder, identified as the A-site size variance $\sigma^2 = \langle r_A^2 \rangle - \langle r_A \rangle^2$ (Ref. 8) is quite large in $Sm_{1-x}Sr_xMnO_3$ ($\sigma^2 \approx 10^{-2}$ Å^2 for $x=0.48$). For such a system with large quenched disorder, the formation energy for lattice polarons is considerably lowered, and when these polarons form in the FM phase the ferromagnetism is truncated, rendering the transition first order.[5,9] As the transition temperature is increased either by applying external magnetic field or pressure or by doping, the tendency for polaron formation decreases and the magnetic transition becomes second order in nature or it becomes a crossover.[9]

In this paper, we have studied the nature of FM to PM phase transition in $Sm_{1-x}Sr_xMnO_3$ with $x=0.48$. The reason why we have chosen $x=0.48$ is that close to half doping ($x=0.5$), FM metal to an antiferromagnetic or charge ordering insulator transition occurs, and when the system is close to MIT, even a weak perturbation such as magnetic field (H), pressure (P), irradiation, and substitution may change the physical properties dramatically or induce a phase transition.[4,10–14] We demonstrate that with the variation in both external (H and P) and internal [y: Nd concentration in $(Sm_{1-y}Nd_y)_{0.52}Sr_{0.48}MnO_3$] parameters $Sm_{0.52}Sr_{0.48}MnO_3$ exhibits a rich magnetic phase diagram. Indeed, our analysis reveals that there exist three critical endpoints at which first-order FM transition truncates.

II. EXPERIMENTAL DETAILS

The single crystals of $(Sm_{1-y}Nd_y)_{0.52}Sr_{0.48}MnO_3$ with $y=0$, 0.05, 0.1, 0.2, and 0.3 have been prepared by floating zone technique. The starting materials, Sm_2O_3, Nd_2O_3, $SrCO_3$, and Mn_3O_4 were mixed in appropriate ratios, heated in air at ~1350 K for 20 h and then pulverized. This procedure was repeated for several times. The resultant powder was formed to cylindrical shape with use of hydrostatic pressure to make a feed rod and then annealed. The apparatus used for crystal growth was the floating zone furnace equipped with two halogen incandescent lamps and hemielliptic focusing mirrors. The feed and seed rods were rotated in opposite directions at 25 rpm. The molten zone was vertically scanned at a rate of 8–10 mm/h in oxygen atmo-

sphere. The quality of the crystal was carefully checked by various techniques such as x-ray powder diffraction, Laue diffraction, electron dispersive x-ray analysis, and scanning electron microscope. The magnetization (M) measurements were done in a superconducting quantum interference device magnetometer [magnetic property measurement system (MPMS), Quantum Design] in fields up to 7 T and in a vibrating sample magnetometer (Oxford Instruments) up to 11.5 T using five-scan averaging. For $M(H)$, the data were collected at 1 to 4 K interval after stabilizing the temperature for about 45 min. Resistivity measurements were performed by a conventional four-probe technique over a wide range of temperature ($T=5-300$ K) for different applied magnetic fields ($H=0-11.5$ T) and hydrostatic pressures ($P=0-2$ GPa). Resistivity under pressure was measured by using a self-clamp-type hybrid hydrostatic pressure cell, and the pressure was monitored using a manganin resistance device. The thermoelectric power has been measured using a differential technique where a small temperature gradient is created across the sample and the voltage developed between the hot and cold ends of the thermocouple formed by the sample and Cu wires is measured using a nanovoltmeter. In the vicinity of FM-PM transition, the temperature difference between the two ends of the sample was kept small. The temperature difference across the sample was measured using a chromel-alumel thermocouple. The sample temperature was controlled with a Si-diode sensor and a manganin heater.[15] All the measurements were performed with a slow sweep rate of temperature and magnetic field.

III. RESULTS AND DISCUSSION

Figure 1(a) shows the temperature dependence of resistivity (ρ) of $Sm_{0.52}Sr_{0.48}MnO_3$ single crystal for different applied magnetic fields. For $H=0$, ρ increases exponentially upon cooling from high temperature and then it suddenly drops as much as 3 orders of magnitude at the MIT along with thermal hysteresis. With increasing field, resistivity substantially decreases, MIT shifts toward the higher temperature, and the width of the hysteresis narrows down progressively. As MIT in manganites is accompanied by FM-PM phase transition, we have also investigated the temperature dependence of magnetization for different H [Fig. 1(b)]. The FM transition is notably sharp at low fields and the sharpness decreases at high fields. The application of magnetic field increases the FM transition temperature (T_C) at the rate of 11.3 K/T up to a field of ~4 T; after that T_C increases at a slower rate. Similar to ρ, M also shows strong hysteresis which diminishes with increasing H. Additionally, we have measured the temperature dependence of thermopower (Q) for different H [Fig. 1(c)]. It is clear that $Q(T)$ below T_C mimics the T dependence of M. At $H=0$, Q increases sharply just below T_C and the sharpness decreases at high fields as in the case of magnetization. The sharp change in ρ, M, and Q at T_C and the presence of thermal hysteresis indicate that the FM transition is first order in nature in the low-field regime, which gets weakened at high fields, as clearly reflected by the suppression of the discontinuity in resistivity, magnetization, and thermopower at the transition and reduction in the hysteresis width.[16]

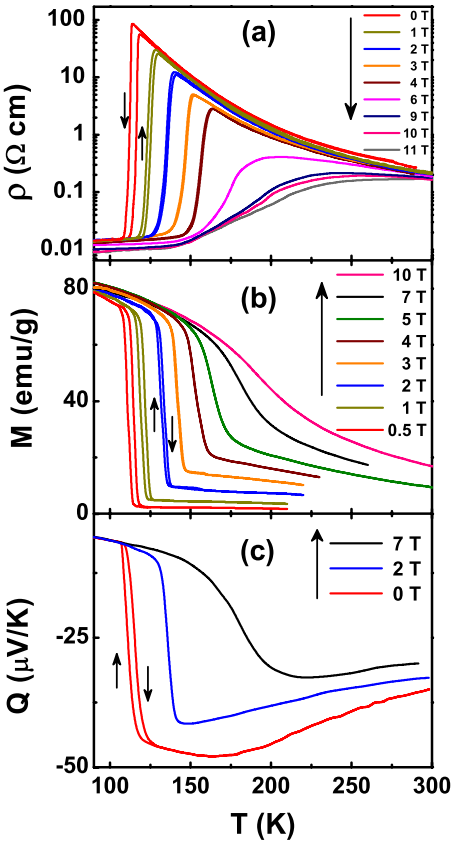

FIG. 1. (Color online) Temperature dependence of (a) resistivity (ρ), (b) magnetization (M), and (c) thermopower (Q) of $Sm_{0.52}Sr_{0.48}MnO_3$ single crystal for different magnetic fields.

For the quantitative analysis, we have calculated the temperature coefficient of magnetization (dM/dT) and resistivity ($d\rho/dT$) in the vicinity of FM to PM transition for different H. The temperature dependence of dM/dT and $d\rho/dT$ curves show a peak at T_C. The peak width at half maximum of $dM/dT(\Delta_{MT})$ and $d\rho/dT(\Delta_{\rho T})$ are plotted as a function of H in Fig. 2(a). Both $\Delta_{MT}-H$ and $\Delta_{\rho T}-H$ curves consist of two straight-line segments that intersect approximately at $H=4$ T. For $H<4$ T, Δ_{MT} and $\Delta_{\rho T}$ are almost independent of H, while above 4 T both of them increase with H. This kind of dependence of Δ_{MT} and $\Delta_{\rho T}$ on H indicates that the nature of FM transition changes at around 4 T.[17] To describe this change more precisely, we have plotted the H dependence of thermal hysteresis width (ΔT), calculated from $M(T)$ and $\rho(T)$ curves [Fig. 2(a)]. The value of ΔT is about 4 K at $H=0$, and it decreases continuously with increasing field and becomes zero above $H=4$ T. This indicates that $H_{cr}=4$ T is a critical field at which the first-order FM transition becomes a crossover. For understanding the nature of magnetic phase transition in manganites, thermopower is also a sensitive tool as it is directly related to the specific heat (C) of charge carriers via $C \propto TdQ/dT$.[18] In Fig. 2(b), we have plotted TdQ/dT as a function of T for different H. The shape and width of TdQ/dT peak for $H=0$ and 2 T are consistent with the first-order phase transition for which there would be a sharp symmetric peak (latent heat), but the λ-like peak corresponding to $H=7$ T is similar to a second-order transition.

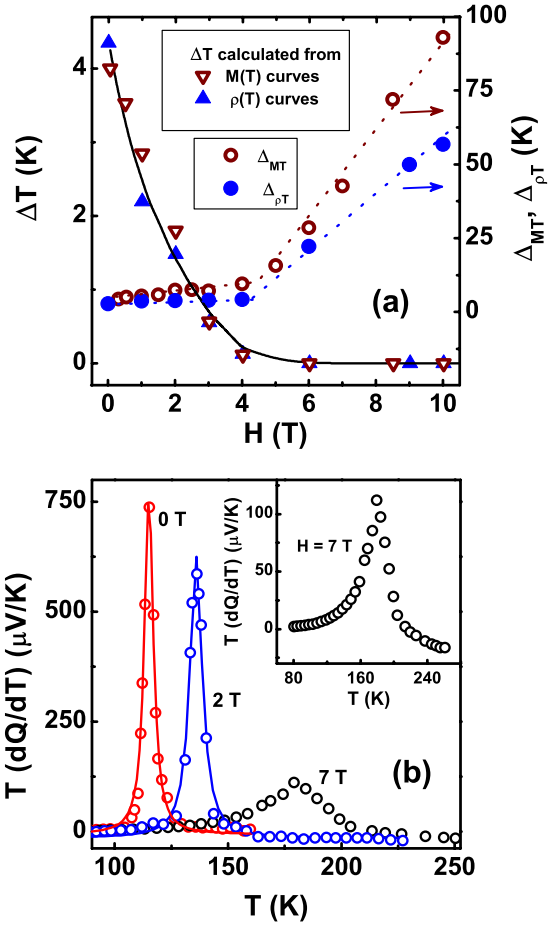

FIG. 2. (Color online) (a) Magnetic field dependence of Δ_{MT}, $\Delta_{\rho T}$, and thermal hysteresis width (ΔT) of resistivity and magnetization. (b) Temperature dependence of TdQ/dT for different fields. The open symbols correspond to experimental data points, and the solid lines represent the Lorentzian fitting. Inset shows the asymmetric nature of the peak of TdQ/dT at $H=7$ T.

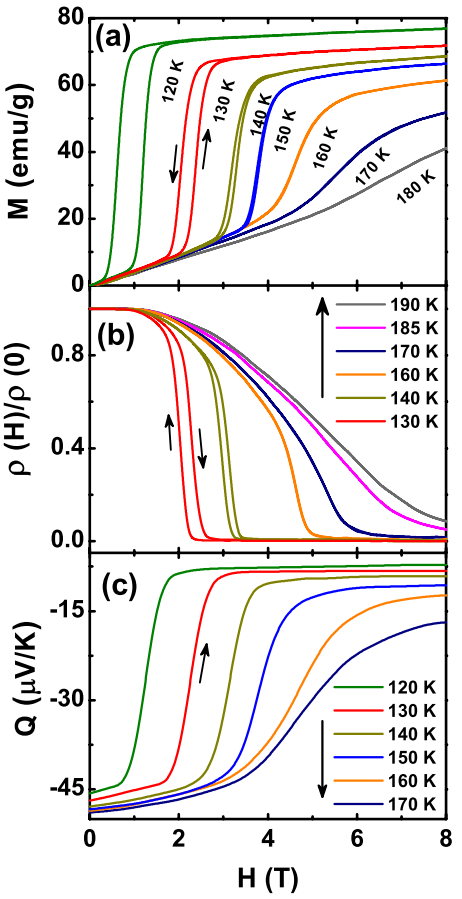

FIG. 3. (Color online) (a) Magnetization (M), (b) resistivity (ρ), and (c) thermopower (Q) of $Sm_{0.52}Sr_{0.48}MnO_3$ single crystal as a function of magnetic field (H) at different constant temperatures.

The data for $H=0$ and 2 T can be fitted well by a Lorentzian function as shown in Fig. 2(b). However, the peak corresponding to $H=7$ T cannot be fitted by the Lorentzian function because of its asymmetric nature [inset of Fig. 2(b)]. Thus, the field dependences of the nature of FM transition described by using magnetization, resistivity, and thermopower data are consistent with each other.

Figure 3(a) shows a series of isotherms of magnetization $M(H)$ for some selected temperatures above T_C ($\approx$110 K at $H=0$). Initially M increases linearly with H up to a transition field above which it suffers a steplike jump. Earlier studies established that the field-induced metamagnetic transition from PM to FM state in this system is due to the formation of inhomogeneous metastable state in the presence of quenched disorder.[4] Such a steplike jump in M and the hysteresis between increasing and decreasing field are the manifestation of first-order PM-FM phase transition as observed in MnAs.[19] With increasing temperature, the sharpness of the jump as well as the width of the hysteresis in $M(H)$ decrease. In Fig. 3(b), the magnetoresistance $[\rho(H)/\rho(0)]$ for $Sm_{0.52}Sr_{0.48}MnO_3$ crystal is also shown. It is clear from the figure that at low fields, the change in magnetoresistance is steep along with hysteresis. Similar to ρ and M, Q also shows a field-induced steplike jump which disappears at high temperatures [Fig. 3(c)]. The field dependences of M, ρ, and Q isotherms suggest that the field-induced first-order PM-FM transition weakens with increasing temperature.

As susceptibility is very sensitive to thermodynamic phase transition, we have plotted the differential susceptibility (dM/dH) as a function of field for various temperatures [inset of Fig. 4(a)]. A clear peak has been observed in each dM/dH vs H curve, which is the indication of PM–FM phase transition with the application of H. The sharpness of the metamagnetic transition can be determined from the width of the peak of dM/dH vs H curve. The full width at half maximum (Δ_{MH}) of dM/dH vs H curve as a function of temperature is shown in Fig. 4(a). Δ_{MH} is almost independent of H below $\sim$160 K, but above that it increases rapidly with H. The width of the hysteresis (ΔH) in $M(H)$ between increasing and decreasing field is about 0.6 T at 120 K, which decreases with increasing temperature and disappears above a critical temperature, $T_{cr}=160$ K [Fig. 4(b)]. Thus, from different perspectives we have shown that ($H_{cr}\approx 4$ T, $T_{cr}\approx 160$ K) is a critical endpoint of first-order FM phase transition in $Sm_{0.52}Sr_{0.48}MnO_3$.

Figure 5(a) shows the temperature dependence of the resistivity of $Sm_{0.52}Sr_{0.48}MnO_3$ crystal at different applied pressures up to 2 GPa. The MIT is quite sharp for $P=0$, and

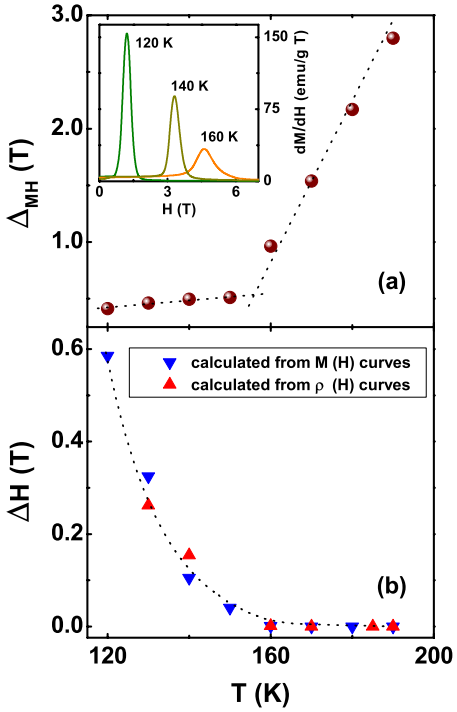

FIG. 4. (Color online) (a) Temperature dependence of Δ_{MH}. Inset: differential susceptibility (dM/dH) as a function of H for some selected temperatures. (b) Temperature dependence of the width of the hysteresis (ΔH) of resistivity and magnetization between increasing and decreasing fields.

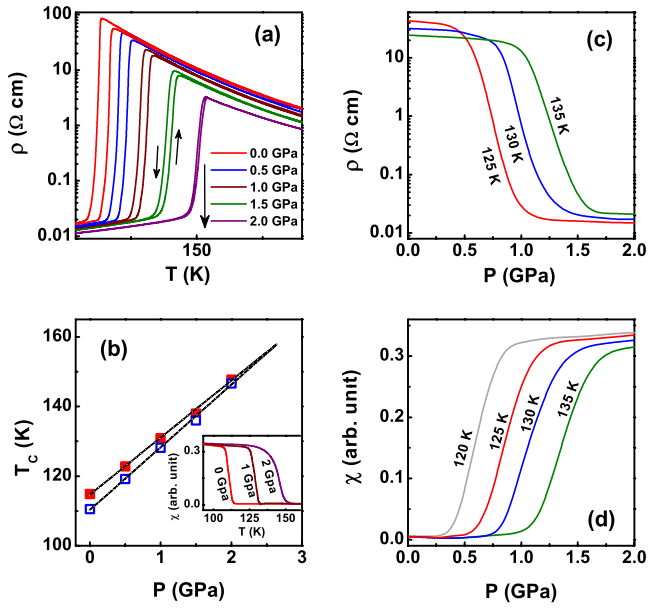

FIG. 5. (Color online) (a) Temperature dependence of resistivity (ρ) of $Sm_{0.52}Sr_{0.48}MnO_3$ single crystal at different hydrostatic pressures (P). (b) Pressure dependence of T_C. Closed and open symbols are the transition temperatures for the heating and cooling cycles, respectively. Inset: temperature dependence of ac susceptibility (χ) for different pressures. P dependence of (c) ρ and (d) χ at different constant temperatures.

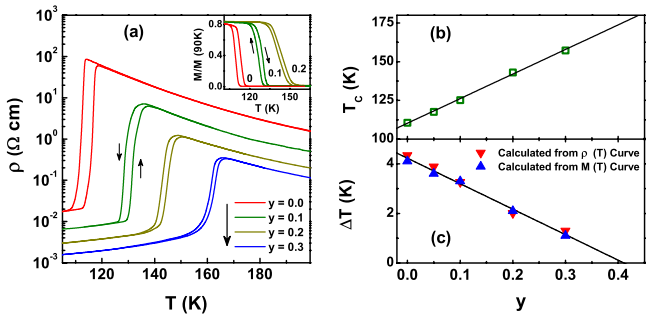

FIG. 6. (Color online) (a) Temperature dependence of resistivity (ρ) of $(Sm_{1-y}Nd_y)_{0.52}Sr_{0.48}MnO_3$ single crystals with $y=0$, 0.1, 0.2, and 0.3. Inset: T dependence of magnetization (M) at $H=500$ Oe for $y=0$, 0.1, and 0.2. (b) y dependence of T_C (for cooling cycle). (c) y dependence of the width of the thermal hysteresis (ΔT) of ρ and M.

the sharpness does not decrease appreciably up to the highest pressure 2 GPa. The application of pressure decreases ρ and shifts T_C toward the higher temperature at the rate of $\sim$19 K/GPa [Fig. 5(b)]. Similar to resistivity, the real part of ac susceptibility (χ) also shows a sharp drop at T_C [inset of Fig. 5(b)]. It is evident from Fig. 5(a) that ρ shows strong thermal hysteresis. With increasing pressure, the width of the thermal hysteresis gradually decreases and the two phase transition lines, corresponding to the heating and cooling cycles, merge to one another at a critical pressure, $P_{cr}=2.5$ GPa and the corresponding T_{cr} is $\sim$160 K [Fig. 5(b)]. This implies that the nature of FM transition in $Sm_{0.52}Sr_{0.48}MnO_3$ changes from first to second order at a critical point ($P_{cr}\approx 2.5$ GPa, $T_{cr}\approx 160$ K). Figures 5(c) and 5(d) show the pressure dependence of ρ and χ for different temperatures below T_{cr}. As pressure increases, ρ shows a sharp drop (almost 3 orders of magnitude) while χ suffers a steplike jump. The sharp change in ρ and χ indicate the first-order nature of PM to FM transition. Thus the external pressure affects the transport and magnetic properties of the present system in a way which is quite similar to that of applied magnetic field and changes the nature of FM transition at the critical point.

Besides the external perturbations like magnetic field and pressure, we have also investigated the effect of internal perturbation, originated due to the substitution of Nd at Sm site, on the nature of the FM transition of $Sm_{0.52}Sr_{0.48}MnO_3$. As the ionic size of Nd is larger than Sm, substitution of Nd at Sm site increases internal chemical pressure of the system. Figure 6(a) shows the temperature dependence of resistivity and magnetization of $(Sm_{1-y}Nd_y)_{0.52}Sr_{0.48}MnO_3$ single crystals for different y. All the $\rho(T)$ curves exhibit MIT at different temperatures similar to that observed in the case of T dependence of ρ at different H and P. Both $\rho(T)$ and $M(T)$ curves exhibit large thermal hysteresis. With increasing y, resistivity decreases and T_C (taken as the temperature at which M and ρ just start to increase) increases almost linearly. One can also observe that the thermal hysteresis width, ΔT, becomes narrower and the discontinuity in $\rho(T)$ at T_C diminishes with increasing y. If both T_C and ΔT continue to change in the same fashion then the hysteresis would vanish just above $y=0.4$ and the corresponding T_C would be

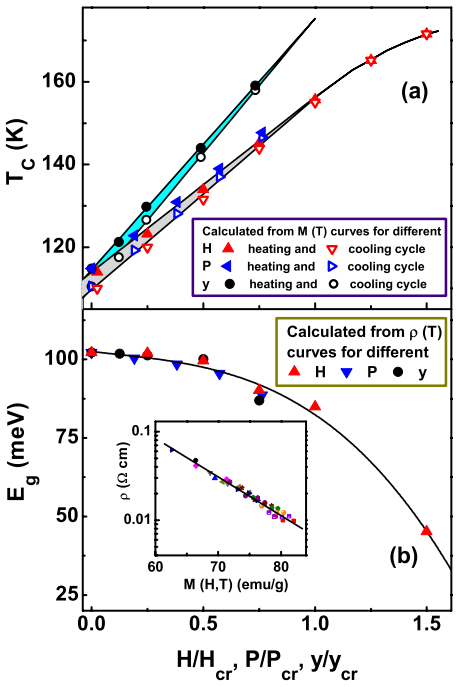

FIG. 7. (Color online) (a) Magnetic phase diagram of $Sm_{0.52}Sr_{0.48}MnO_3$: T_C as functions of H, P, and y, normalized with respect to their critical values. (b) H, P, and y dependence of the activation energy (E_g). Inset: $\rho(H,T)$ vs $M(H,T)$ of $Sm_{0.52}Sr_{0.48}MnO_3$ for various T ranging from 90 to 150 K in 5 K interval. At each T, points are included for H=0.05, 1.0, 2.0, 3.0, and 4.0 T. The solid line is a linear fit to the data.

~175 K [Figs. 6(b) and 6(c)]. This behavior indicates that the first-order FM transition in $Sm_{0.52}Sr_{0.48}MnO_3$ changes to second order with Nd doping above a critical point ($y_{cr} \approx 0.4$, $T_{cr} \approx 175$ K). In this context we would like to mention that the effects of external H and P on the nature of FM transition for different y below y_{cr} have also been examined. Similar behavior is observed as in the case of y=0 sample, i.e., first-order FM transition truncates at the critical point. However, the values of H_{cr} and P_{cr} decrease monotonically with increasing y.

The magnetic phase diagram in terms of the evolution of T_C as functions of different perturbations (H, P, and y), normalized with respect to their critical values (H_{cr}, P_{cr} and y_{cr}), is shown in Fig. 7(a). With the decrease in the strength of perturbations, the phase transition curve splits into two lines: one of them corresponds to the FM to PM phase transition, which occurs on heating, while the other corresponds to the inverse transition from PM to FM phase that occurs on cooling. In the shaded region, the magnetic state of the system is determined by the way through which the sample arrives at this region, i.e., by the increase or decrease in temperature. This confirms that the system has the critical endpoint at which first-order FM transition becomes second order or crossover under the influence of both external and internal perturbations. The change in the magnetic phase transition with the variation in different parameters can be explained on the basis of the formation of polarons—charge carriers accompanied by a localized distortion of the surrounding crystal lattice.[9,20–22] The possibility for the existence of polarons comes from the activated semiconductorlike behavior of ρ [$\rho \sim \exp(E_g/kT)$, where E_g is the activation energy] above T_C. To fully understand more, we have plotted ρ as a function of M for different H and T and found that ρ, just below T_C, is related to M through the phenomenological relation $\rho(H,T)=\rho_m \exp[-M(H,T)/M_0]$, where ρ_m and M_0 are constants [inset of Fig. 7(b)].[21] This ρ-M correlation suggests that the polaronic hopping is the prevalent conduction mechanism below T_C. For temperatures above T_C, where FM fluctuation is not observed and the system is in PM state ($M \propto H$), ρ and M are no longer related by the above relation. The existence of polarons can also be detected from the combination of lattice parameters, magnetic susceptibility, and neutron-scattering measurements.[22] The sharp volume contraction as the temperature is lowered to T_C, the large neutron-scattering intensity, and the deviation of susceptibility from the Curie-Weiss behavior just above T_C have been observed in $Sm_{0.52}Sr_{0.48}MnO_3$.[23,24] All these features can be interpreted coherently by assuming that the observed lattice distortions and magnetic clusters are caused by the same entity—the polaron.[22] When these polarons form, self-trapping becomes more evident and drives the material toward a first-order phase transition. For understanding the role of H, P, and y on the formation of polarons, we have calculated E_g from the slope of $\ln(\rho)$ vs $1/T$ curve. In Fig. 7(b), E_g is plotted as functions of H, P, and y. At ambient condition, the value of E_g is 102 meV. As the strength of these perturbations increases, E_g decreases monotonically. This behavior indicates that magnetic field, pressure, and substitution of Nd suppress the formation of polaronic state and increase the bandwidth of the system, and as a consequence first-order FM-PM transition becomes second order or crossover in nature.[20]

It is evident from Fig. 7(a) that the magnetic phase diagram strongly depends on the nature of the applied perturbation. Both of the external perturbations H and P give rise to the nearly identical phase diagram but it differs if the perturbation is internal. This may be better understood by comparing the value of external pressure with the internal pressure (P_{int}), arising due to the substitution of Nd. It has been shown that by varying the average ionic radius by $\Delta\langle r_A\rangle$, P_{int} can be varied by an amount $\Delta P_{int}=\Delta\langle r_A\rangle/\beta$, where the scaling factor β is 3.7×10^{-3} Å/GPa.[11] The value of P_{int} at y_{cr} =0.4 where the FM transition changes from first-order to second order is 1.6 GPa. This is quite different from the external pressure (P_{cr}=2.5 GPa) at which the order of the FM transition changes. Had T_C enhancement been solely due to the increase in average ionic radius $\langle r_A\rangle$, one would expect that T_C should be 140 K instead of 175 K for y=0.4. It follows that the scaling relation which is applicable for several manganites fails in the present system.[25] This discrepancy can be explained by taking into account the role of A-site size variance (σ^2). In manganites, both $\langle r_A\rangle$ and σ^2 are crucial factors in determining T_C; T_C increases with the decreases in σ^2 (Ref. 8). When Nd is substituted at Sm site, $\langle r_A\rangle$ increases and σ^2 decreases. For y=0.4, $\langle r_A\rangle$ increases by only ~0.5% whereas σ^2 decreases by ~10%.

IV. CONCLUSION

In conclusion, the nature of FM to PM phase transition in $Sm_{0.52}Sr_{0.48}MnO_3$ single crystal has been studied by trans-

port and magnetic measurements. At ambient condition, the sharp change in resistivity, thermopower, and magnetization at T_C, along with thermal hysteresis, clearly indicates that the nature of FM transition in $Sm_{0.52}Sr_{0.48}MnO_3$ is first order. External magnetic field, pressure, and substitution of Nd at Sm site increase T_C, reduce the tendency of polaron formation, and thus change the FM transition to second order in nature or it becomes a crossover at the critical points. We have identified the location of three such critical points expressed in terms of H, P, and y and are given by ($H_{cr} \approx 4$ T, $T_{cr} \approx 160$ K), ($P_{cr} \approx 2.5$ GPa, $T_{cr} \approx 160$ K), and ($y_{cr} \approx 0.4$, $T_{cr} \approx 175$ K).

*prosenjit.sarkar@saha.ac.in

[1] Y. Tokura, Rep. Prog. Phys. **69**, 797 (2006).
[2] E. Dagotto, T. Hotta, and A. Moreo, Phys. Rep. **344**, 1 (2001).
[3] Y. Tomioka and Y. Tokura, Phys. Rev. B **70**, 014432 (2004).
[4] L. M. Fisher, A. V. Kalinov, I. F. Voloshin, N. A. Babushkina, D. I. Khomskii, Y. Zhang, and T. T. M. Palstra, Phys. Rev. B **70**, 212411 (2004).
[5] T. J. Sato, J. W. Lynn, and B. Dabrowski, Phys. Rev. Lett. **93**, 267204 (2004).
[6] P. Sarkar, P. Mandal, A. K. Bera, S. M. Yusuf, L. S. Sharath Chandra, and V. Ganesan, Phys. Rev. B **78**, 012415 (2008).
[7] K. Mydeen, P. Sarkar, P. Mandal, A. Murugeswari, C. Q. Jin, and S. Arumugam, Appl. Phys. Lett. **92**, 182510 (2008).
[8] L. M. Rodriguez-Martinez and J. P. Attfield, Phys. Rev. B **54**, R15622 (1996); **63**, 024424 (2000).
[9] M. B. Salamon and M. Jaime, Rev. Mod. Phys. **73**, 583 (2001).
[10] Y. Tokura, H. Kuwahara, Y. Moritomo, Y. Tomioka, and A. Asamitsu, Phys. Rev. Lett. **76**, 3184 (1996).
[11] H. Y. Hwang, T. T. M. Palstra, S. W. Cheong, and B. Batlogg, Phys. Rev. B **52**, 15046 (1995).
[12] V. Kiryukhin, D. Kasa, J. P. Hill, B. Keimer, A. Viglante, Y. Tomioka, and Y. Tokura, Nature (London) **386**, 813 (1997).
[13] N. A. Babushkina, E. A. Chistotina, O. Y. Gorbenko, A. R. Kaul, D. I. Khomskii, and K. I. Kugel, Phys. Rev. B **67**, 100410(R) (2003).
[14] L. Demkó, I. Kézsmárki, G. Mihály, N. Takeshita, Y. Tomioka, and Y. Tokura, Phys. Rev. Lett. **101**, 037206 (2008).
[15] J. B. Mandal, S. Keshri, P. Mandal, A. Poddar, A. N. Das, and B. Ghosh, Phys. Rev. B **46**, 11840 (1992).
[16] S. W. Biernacki, Phys. Rev. B **68**, 174417 (2003).
[17] R. I. Zainullina, N. G. Bebenin, V. V. Ustinov, Y. M. Mukovskii, and D. A. Shulyatev, Phys. Rev. B **76**, 014408 (2007).
[18] S. H. Tang, P. P. Craig, and T. A. Kitchens, Phys. Rev. Lett. **27**, 593 (1971).
[19] C. P. Bean and D. S. Rodbell, Phys. Rev. **126**, 104 (1962).
[20] R. M. Kusters, J. Singleton, D. A. Keen, R. M. Greevy, and W. Hayes, Physica B **155**, 362 (1989).
[21] M. F. Hundley, M. Hawley, R. H. Heffner, Q. X. Jia, J. J. Neumeier, J. Tesmer, J. D. Thompson, and X. D. Wu, Appl. Phys. Lett. **67**, 860 (1995).
[22] J. M. De Teresa, M. R. Ibarra, P. A. Algarabel, C. Ritter, C. Marquina, J. Blasco, J. Garcia, A. Del Moral, and Z. Arnold, Nature (London) **386**, 256 (1997).
[23] Y. Tomioka, H. Hiraka, Y. Endoh, and Y. Tokura, Phys. Rev. B **74**, 104420 (2006).
[24] P. Sarkar and P. Mandal, Appl. Phys. Lett. **92**, 052501 (2008).
[25] P. Postorino, A. Congeduti, P. Dore, A. Sacchetti, F. Gorelli, L. Ulivi, A. Kumar, and D. D. Sarma, Phys. Rev. Lett. **91**, 175501 (2003).